

УДК 544.653. 2/.3

**Perovskite-like  $(\text{La}_{0.75}\text{Ca}_{0.25})_{0.95}\text{Cr}_{1-x}\text{Fe}_x\text{O}_{3-\delta}$  as potential electrode materials for symmetric Solid Oxide Fuel Cells**

V.A. Kolotygin, A.I. Ivanov, N.B. Kostretsova, V.V. Kharton

*Institute of Solid State Physics RAS, Chernogolovka, Moscow District, 2 Academician*

*Ossipyan str., 142432 Russia*

*kolotygin@issp.ac.ru*

**Annotation**

The study is centered on the synthesis and characterization of  $(\text{La}_{0.75}\text{Ca}_{0.25})_{0.95}\text{Cr}_{1-x}\text{Fe}_x\text{O}_{3-\delta}$  ( $x = 0.3 - 0.9$ ) perovskites as potential materials for solid oxide fuel cell (SOFC) cathode and anode. These materials possess an orthorhombically-distorted structure at room temperature whilst heating above 800-1100 K induces reversible transformation into the rhombohedral symmetry. The transition temperature increases with iron content. The linear thermal expansion coefficients vary in the range  $(10.5-11.1) \times 10^{-6} \text{ K}^{-1}$  and slightly increase on Fe doping. The volume changes upon reduction are within 0.16%. The electronic conductivity exhibits a thermally-activated character and increases on Fe introduction, in particular due to increasing number of the sites available for the electronic transfer; this trend is observed both under oxidizing and reducing conditions. The low level of the electronic conductivity seems to be responsible for an insufficient electrochemical activity of  $(\text{La}_{0.75}\text{Ca}_{0.25})_{0.95}\text{Cr}_{1-x}\text{Fe}_x\text{O}_{3-\delta}$ -based cathodes. Under anodic conditions other factors, such as electrode microstructure or surface-related properties, affect the electrochemical behavior.

**Keywords:** perovskite, phase transition, thermal expansion, chemical expansion, total conductivity, polarization resistance.

**Introduction**

Reducing operation temperature of Solid Oxide Fuel Cells (SOFC) and a partial replacement of hydrogen by other fuels, generally produced from hydrocarbon-containing sources, requires development of novel functional materials capable to adequately operate under necessary conditions. Conventional Ni-based composites used as SOFC anodes suffer from microstructural degradation with time or upon redox cycling and possible coking in hydrocarbon- or carbon monoxide-enriched atmospheres [1-3]. Chromite-based perovskites are

considered to be possible alternative anode materials due to their high stability under reducing conditions and moderate volume and microstructural changes on reduction which decreases the risk of the electrode cracking or delamination from the solid electrolyte. However, significant limitation of  $\text{LaCrO}_{3-\delta}$  and related materials is their insufficient conductivity, especially under reducing conditions, and low electrochemical activity towards oxidation processes which requires addition of surface-active agents into the anode layer [2, 4-6].

In recent 15-20 years it was demonstrated that appropriate doping in A- or B-sublattice may substantially improve the electrode properties of chromites both in oxidizing and reducing atmospheres. The latter factor is attractive for their simultaneous utilization as cathodes and anodes in symmetrical SOFCs where both electrodes are prepared from the same material which simplifies the procedure of the electrode coating and subsequent firing [5, 7-11]. The basic strategy of substitution in B-sublattice relates to introducing cations with variable oxidation state or oxygen coordination (Mn, Fe, Co, Ni, V) which allows to generate additional charge carriers and channels of their transfer, improve the oxygen ionic conductivity due to higher concentration of oxygen vacancies or modify the surface-related properties. In particular,  $(\text{La,Sr})(\text{Cr,Mn})\text{O}_{3-\delta}$  perovskites are considered to be among the most active Ni-free anode materials due to the comparatively high performance in  $\text{H}_2$ , hydrocarbons, alcohols and other fuels [5, 11-14]. Due to the high stability and acceptable conductivity in both oxidizing and reducing atmospheres, this material has a great potential for utilization as both electrodes of symmetrical SOFCs [8, 12, 15].

Fe-doped chromites represent another attractive group of perovskite-based anodes since these materials combine both acceptable stability in the anode atmosphere and the conductivity level necessary for ensuring good anode properties. In particular, in [7, 8] the performance of  $(\text{La,Sr})(\text{Cr,Fe})\text{O}_{3-\delta}$  anodes was demonstrated to be superior compared to that of Mn-substituted analogues measured under similar conditions, while the low-temperature stabilization of the oxygen nonstoichiometry enables to preserve a comparatively high conductivity level (40-50 S/cm) even in reducing atmospheres.  $(\text{La,Sr})(\text{Cr,Fe})\text{O}_3$ -based anodes demonstrated moderate performance in hydrocarbon-, CO-,  $\text{H}_2\text{S}$ - and even  $\text{PH}_3$ -containing fuels, with more stable operation compared to conventional Ni-based anodes [10, 16-19]. However, Fe-doped chromites are reported to exhibit an enormous expansivity ( $>1\%$  in linear scale [7]) upon reduction which may be problematic for long-term utilization of the corresponding cell.

Previous studies on  $(\text{La,Sr,Ca})\text{FeO}_{3-\delta}$  perovskites demonstrated that a partial or complete substitution of Ca for Sr allows to modify the functional properties, particularly, to reduce the thermal and chemical expansion and to some extent improve the phase stability. Excessive

amount of Ca is undesirable since it may lead to ordering of oxygen vacancies in the crystal lattice deteriorating the transport properties; this effect is substantially suppressed for Cr-containing ferrites [20-22]. Taking the above information into account, the present work is focused on evaluation of  $(\text{La}_{0.75}\text{Ca}_{0.25})_{0.95}\text{Cr}_{1-x}\text{Fe}_x\text{O}_{3-\delta}$  ( $0.3 \leq x \leq 0.9$ ) perovskites as potential cathode and anode materials of symmetrical SOFCs.

## Purpose of the article

The primarily goal of the work is to study the phase and structural stability, transport and thermomechanical properties of  $(\text{La}_{0.75}\text{Ca}_{0.25})_{0.95}\text{Cr}_{1-x}\text{Fe}_x\text{O}_{3-\delta}$  perovskites and evaluate the electrochemical activity of the corresponding cathodes and anodes, with a particular emphasis on the relationships between the transport, electrochemical and structural behavior of these materials.

## Experimental

Synthesis of  $(\text{La}_{0.75}\text{Ca}_{0.25})_{0.95}\text{Cr}_{1-x}\text{Fe}_x\text{O}_{3-\delta}$  (LCCF) solid solutions was carried out with glycine-nitrate processing (GNP) from  $\text{La}(\text{NO}_3)_3 \cdot 6\text{H}_2\text{O}$ ,  $\text{Ca}(\text{NO}_3)_2$ ,  $\text{Cr}(\text{NO}_3)_3 \cdot 9\text{H}_2\text{O}$  and  $\text{FeC}_2\text{O}_4 \cdot 2\text{H}_2\text{O}$  preliminary dissolved in 20 mL of concentrated nitric acid as precursors. The precise molar mass of the starting reactants which might be affected by possible water losses or other compositional changes with time, was determined with thermogravimetric analysis (TGA) by high-temperature transformation of the corresponding precursor into  $\text{La}_2\text{O}_3$ ,  $\text{CaO}$  or  $\text{Fe}$  in air or  $\text{H}_2$ -Ar atmosphere until the constant mass was achieved. The water content was calculated from the relative mass changes. The details of the GNP method may be found elsewhere ([7, 12] and references cited). The synthesized powder was consecutively grinded in a mortar and annealed in a furnace at 1073 – 1573 K. In order to obtain dense ceramics, the annealed powders were uniaxially compacted in a press mould under 100-150 MPa pressure followed by sintering at 1673 – 1743 K in air.

X-ray diffraction (XRD) analysis was carried out with a Siemens D-500-BRAUN diffractometer using of  $\text{CuK}_\alpha$  irradiation in the  $2\theta$  range of 20-80 °. The analysis of the phase composition and calculation of the lattice parameters was made with Match and PowderCell 2.4 software. Studies of the transport and thermomechanical properties were performed on rectangular-shaped bars obtained by cutting and subsequent polishing of the ceramic pellets. The total conductivity was measured on direct current using a 4-probe technique in a laboratory-made tubular furnace in a flow of the required gas; the oxygen partial pressure ( $p(\text{O}_2)$ ) was controlled

using an electrochemical oxygen sensor inserted into the tube. Thermomechanical measurements were fulfilled in a vertical dilatometer Linseis V75 equipped with an electrochemical pump and sensor for ensuring the necessary oxygen content in the gas atmosphere. The methodology of dilatometric measurements and calculation of the thermal/chemical expansion coefficients is discussed in [12, 22] and referenced therein.

Electrochemical properties were studied on symmetrical cells LCCF / LDC / LSGM / LDC / LCCF, where LSGM and LDC correspond to  $(\text{La}_{0.9}\text{Sr}_{0.1})_{0.98}\text{Ga}_{0.8}\text{Mg}_{0.2}\text{O}_{3-\delta}$  and  $\text{Ce}_{0.6}\text{La}_{0.4}\text{O}_{2-\delta}$  used as the solid electrolyte and protective sublayer, respectively. For deposition of the porous electrode layers on LSGM pellet (thickness 0.7-1.0 mm, area 0.4 – 0.5 cm<sup>2</sup>) a laboratory-made print-screening device was used. Each coating step was followed by firing the applied layers in air at 1473 K. The polarization resistance measurements were carried out by a 2-electrode method in a symmetrical configuration, without applying current. Pt meshes were used as current collectors; no additional modifications of the electrodes such as preparation of composites, impregnation with catalytically active agents or coating with a metallic paste were undertaken in the framework of the present study. The studies were carried out in a tubular furnace in O<sub>2</sub>-air-Ar or H<sub>2</sub>-Ar-H<sub>2</sub>O mixtures using an oxygen sensor for p(O<sub>2</sub>) control. The impedance spectra were collected using a potentio-/galvanostat Metrohm Autolab (PGSTAT302N) in 1 MHz – 5 mHz frequency range, with AC amplitude of 50-100 mV. The microstructure of the electrode layers was studied using a LEO SUPRA 50VP (Carl Zeiss, Germany) scanning microscope.

## Results and discussion

Fig. 1 demonstrates XRD patterns of as-prepared  $(\text{La}_{0.75}\text{Ca}_{0.25})_{0.95}\text{Cr}_{1-x}\text{Fe}_x\text{O}_{3-\delta}$ . All the materials synthesized are nearly single-phase perovskites with the orthorhombic structure while reduction of Fe-enriched compositions promotes the transition into the cubic symmetry. Doping with Fe increases the cell parameters (Table 1), in accordance with larger radii of Fe<sup>3+</sup> and Fe<sup>4+</sup> cations compared to chromium analogues [23]. Moreover, substitution of iron for chromium might enhance the oxygen deficiency leading to increasing the ratio of 3-fold charged cations to 4-fold ones; this fact requires verification by measuring the oxygen content under ambient conditions or studying the cation state by X-ray photoelectron spectroscopy, Mössbauer spectroscopy or other appropriate techniques. The same factors might be responsible for a slight increment of the thermal expansion coefficients with iron content (Fig. 2, Table 1).

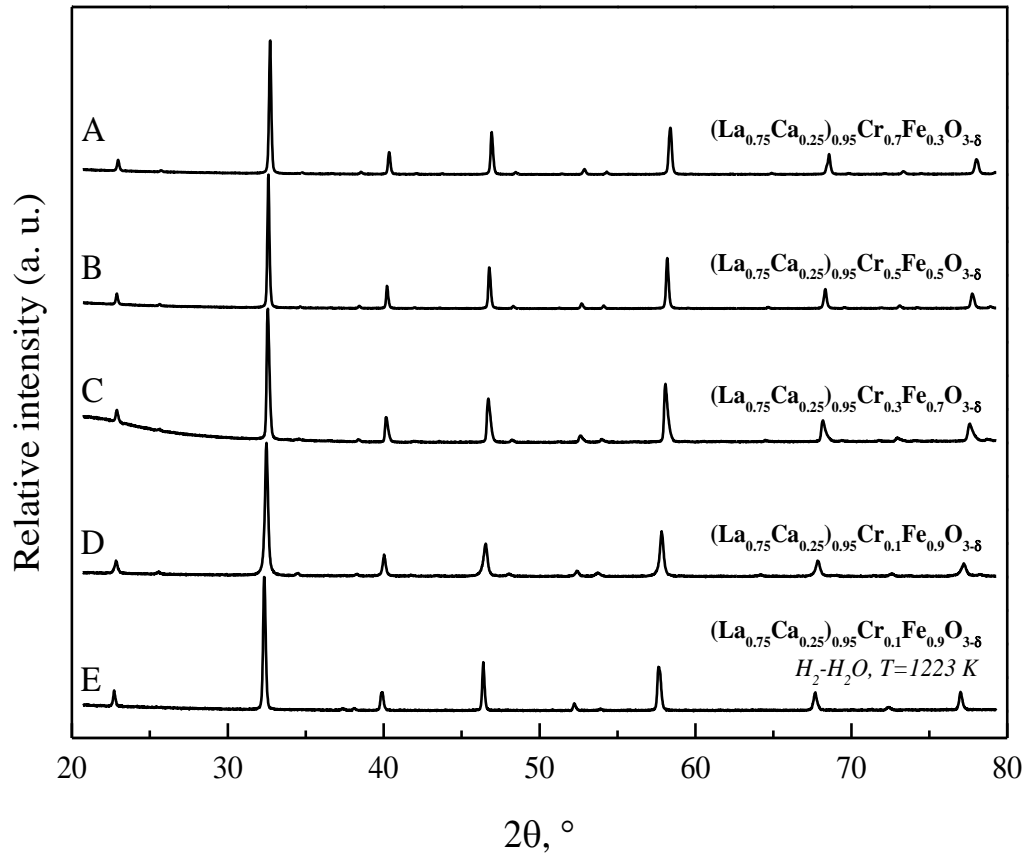


Fig. 1. XRD patterns of  $(\text{La}_{0.75}\text{Ca}_{0.25})_{0.95}\text{Cr}_{1-x}\text{Fe}_x\text{O}_{3-\delta}$  perovskites, slowly cooled in air (A-D) and annealed in humidified 4%  $\text{H}_2$ -Ar (E).

One should note that the effect of iron content on the chemical expansion is different to common trends known for ferrites where replacement of iron with foreign cations generally reduces the oxygen losses and resultant volume changes [7, 24, 25]. The abnormal behavior detected in the present study might be associated with the structural transformation discussed below occurring in the considered temperature range, or with a comparatively high oxygen nonstoichiometry for Fe-enriched compositions in air at elevated temperatures, and subsequent reduction might lead to somewhat lower changes of the oxygen content compared to that of nearly stoichiometric compositions with lower iron content. One should also take into account that the difference in the expansivity is rather small and comparable to the measurement uncertainty. Whatever the origins of the unusual behavior, the volume changes on reduction in  $\text{CO-CO}_2$  atmosphere are 0.10-0.16% in the linear scale which is substantially lower compared to the values reported for  $(\text{La}_{0.75}\text{Sr}_{0.25})_{0.95}\text{Cr}_{1-x}\text{Fe}_x\text{O}_{3-\delta}$  [7] and much closer to the typical level of isothermal expansion of chromite-based materials upon reduction [12, 24-26].

Table 1. Unit cell parameters, thermal expansion coefficients and chemical expansion on reducing of air-prepared  $(\text{La}_{0.75}\text{Ca}_{0.25})_{0.95}\text{Cr}_{1-x}\text{Fe}_x\text{O}_{3-\delta}$  ceramics in CO-CO<sub>2</sub> atmospheres ( $p(\text{O}_2) = 10^{-12} - 10^{-20}$  atm)

Composition	a, Å	b, Å	c, Å	V, Å <sup>3</sup>	TEC×10 <sup>6</sup> , K <sup>-1</sup>	$\frac{L_{\text{air}} - L_{\text{CO/CO}_2}}{L_{\text{air}}}, \%$ (T, K)
$(\text{La}_{0.75}\text{Ca}_{0.25})_{0.95}\text{Cr}_{0.7}\text{Fe}_{0.3}\text{O}_{3-\delta}$ <i>as-prepared in air</i>	5.477(2)	7.745(2)	5.465(2)	231.8 (2)	10.5±0.1	0.13 (1223) 0.16 (973)
$(\text{La}_{0.75}\text{Ca}_{0.25})_{0.95}\text{Cr}_{0.5}\text{Fe}_{0.5}\text{O}_{3-\delta}$ <i>as-prepared in air</i>	5.490(2)	7.765(2)	5.479(2)	233.5 (2)	10.8±0.1	0.13 (1223) 0.14 (973)
$(\text{La}_{0.75}\text{Ca}_{0.25})_{0.95}\text{Cr}_{0.3}\text{Fe}_{0.7}\text{O}_{3-\delta}$ <i>as-prepared in air</i>	5.504(2)	7.787(2)	5.487(2)	235.2 (2)	10.7±0.1	0.11 (1223) 0.10 (973)
$(\text{La}_{0.75}\text{Ca}_{0.25})_{0.95}\text{Cr}_{0.1}\text{Fe}_{0.9}\text{O}_{3-\delta}$ <i>as-prepared in air</i>	5.527(2)	7.833(2)	5.524(2)	239.2 (2)	11.1±0.1	
$(\text{La}_{0.75}\text{Ca}_{0.25})_{0.95}\text{Cr}_{0.1}\text{Fe}_{0.9}\text{O}_{3-\delta}$ <i>reduced in wet H<sub>2</sub>-Ar, 1273 K</i>	3.914(2)			1/4×239.8 (4)		

Cell parameters correspond to the orthorhombic (*Pnma*) or cubic (*Pm3m*) structure for the samples prepared in air or annealed in wet H<sub>2</sub>-Ar, respectively.  $p(\text{O}_2)$  in CO-CO<sub>2</sub> mixture was  $\sim 10^{-13}$  atm (1223 K) and  $\sim 10^{-19}$  atm (973 K). TEC values correspond to the 300-1273 K temperature range in air.

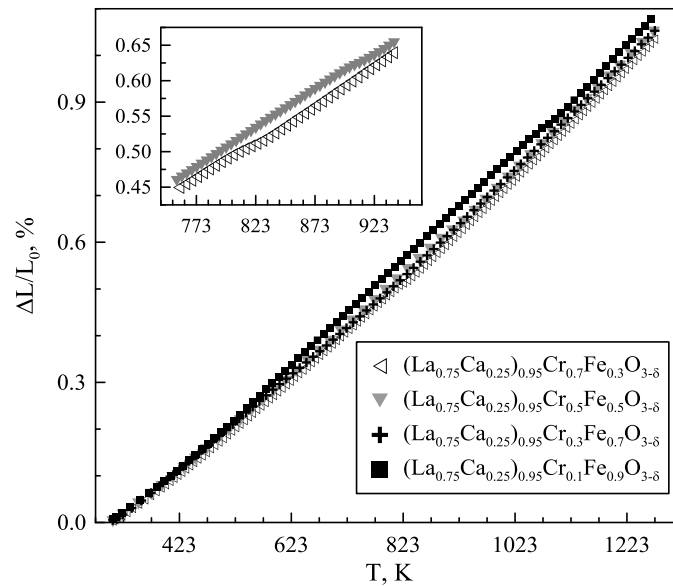


Fig. 2. Relative length changes of  $(\text{La}_{0.75}\text{Ca}_{0.25})_{0.95}\text{Cr}_{1-x}\text{Fe}_x\text{O}_{3-\delta}$  ceramics on cooling in air. The inset shows zoomed view of the dilatometric curves in the 743-953 K temperature range.

A peculiarity of the studied materials is the presence of a kink on the dilatometric curves (inset in Fig. 2) which is reproducible upon heating and cooling runs both in air and argon atmospheres. In accordance with literature data [4, 26-30], this behavior might be associated with reversible 1<sup>st</sup> order transition of the orthorhombic structure into the rhombohedral one. For the title materials, this effect occurs at significantly higher temperatures compared to some other chromites listed in Table 2 which might originate from increasing the transition temperatures upon Ca- or Fe-doping; the effect of Fe introduction on the transition temperature confirms this suggestion. Verification of the structural changes requires high-temperature XRD analysis; nevertheless, from the viewpoint of potential application of the materials as SOFC electrodes, the negligible volume changes induced by this effect as well as moderate chemical expansivity and the values of TECs comparable to those of typical electrolytes [31] suggest an adequate mechanical compatibility between the electrochemical cell components.

Table 2. Comparison of the phase transition temperatures for selected LaCrO<sub>3</sub>-based perovskites

Composition	T <sub>ph.trans</sub> , K	Reference
LaCrO <sub>3-δ</sub>	520	[27, 28]
	560	[29]
La <sub>0.9</sub> Ca <sub>0.1</sub> CrO <sub>3-δ</sub>	580	[27]
La <sub>0.9</sub> Sr <sub>0.1</sub> CrO <sub>3-δ</sub>	340	[27]
LaCr <sub>0.9</sub> Mg <sub>0.1</sub> O <sub>3-δ</sub>	600	[27]
LaCr <sub>0.8</sub> Mg <sub>0.2</sub> O <sub>3-δ</sub>	620	[27]
(La <sub>0.9</sub> Sr <sub>0.1</sub> ) <sub>0.98</sub> Cr <sub>0.9</sub> Mg <sub>0.1</sub> O <sub>3-δ</sub>	336±10	[26]
(La <sub>0.75</sub> Ca <sub>0.25</sub> ) <sub>0.95</sub> Cr <sub>0.7</sub> Fe <sub>0.3</sub> O <sub>3-δ</sub>	815±5	This work
(La <sub>0.75</sub> Ca <sub>0.25</sub> ) <sub>0.95</sub> Cr <sub>0.5</sub> Fe <sub>0.5</sub> O <sub>3-δ</sub>	910±5	This work
(La <sub>0.75</sub> Ca <sub>0.25</sub> ) <sub>0.95</sub> Cr <sub>0.1</sub> Fe <sub>0.9</sub> O <sub>3-δ</sub>	1080±5	This work
(La <sub>0.9</sub> Sr <sub>0.1</sub> ) <sub>0.98</sub> Cr <sub>0.8</sub> Mg <sub>0.1</sub> Fe <sub>0.1</sub> O <sub>3-δ</sub>	405±10	[26]
(La <sub>0.9</sub> Sr <sub>0.1</sub> ) <sub>0.98</sub> Cr <sub>0.6</sub> Mg <sub>0.1</sub> Fe <sub>0.3</sub> O <sub>3-δ</sub>	545±5	[26]
LaCr <sub>0.9</sub> Ni <sub>0.1</sub> O <sub>3-δ</sub>	640	[28]
LaCr <sub>0.8</sub> Ni <sub>0.2</sub> O <sub>3-δ</sub>	670	[28]
(La <sub>0.9</sub> Sr <sub>0.1</sub> ) <sub>0.95</sub> Cr <sub>0.85</sub> Mg <sub>0.1</sub> Ni <sub>0.05</sub> O <sub>3-δ</sub>	360±10	[30]

Increasing iron content leads to an enhancement of the total conductivity; this trend is observed both in air and in wet H<sub>2</sub>-Ar (Fig. 3) and contradicts to the results obtained for (La<sub>0.75</sub>Sr<sub>0.25</sub>)<sub>0.95</sub>Cr<sub>1-x</sub>Fe<sub>x</sub>O<sub>3-δ</sub> [7]. Whereas in the latter case the negative effect of iron content on the conductivity was attributed to its essentially constant oxidation state irrespective to Cr:Fe ratio which suggests exclusion of Fe species from participation in the electron transfer, in the studied materials the conductivity seems to be governed by other factors.

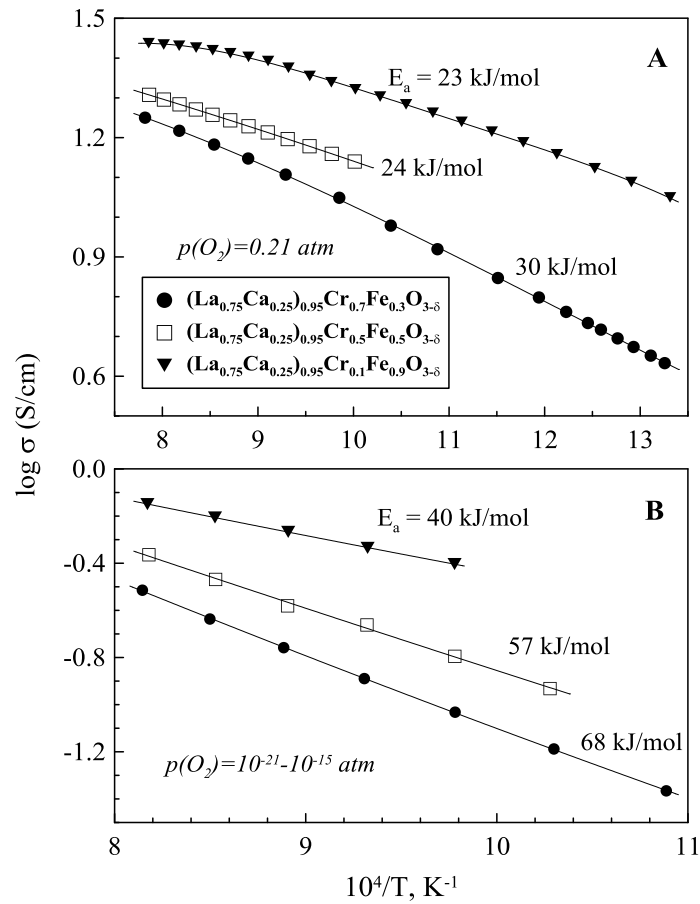


Fig. 3. Temperature dependencies of the total conductivity of (La<sub>0.75</sub>Ca<sub>0.25</sub>)<sub>0.95</sub>Cr<sub>1-x</sub>Fe<sub>x</sub>O<sub>3-δ</sub> ceramics in air (A) and in wet 4% H<sub>2</sub>-Ar mixture (B). The activation energies of the total conductivity are marked near the corresponding data.

One should note that similar contradictions are quite typical for chromite-based materials [5, 32-35] and may be associated with specific factors such as large differences in energy levels between Cr<sup>3+</sup> and guest cations significantly affecting the probability of residence of the charge carriers on these atoms or percolation between the species with close energies which is affected by oxygen nonstoichiometry, lattice symmetry, cell parameters, etc. The conductivity of



$(\text{La}_{0.75}\text{Sr}_{0.25})_{0.95}\text{Cr}_{1-x}\text{Fe}_x\text{O}_{3-\delta}$  exhibits a thermally-activated character; the activation energies decrease with iron content (Fig. 3) suggesting that the electronic transport of presumably p-type electronic charge carriers proceeds more rapidly via Fe-O-Fe channels. For  $x=0.9$ , a slight tendency towards a conductivity maximum typical for ferrite-based materials [21, 24] is observed in air at high temperatures (Fig. 3a) associated with increasing oxygen nonstoichiometry leading to lower concentration of the charge carriers and breaking the conductive channels. The conductivity varies in the range of 10-30 and 0.1-1 S/cm under cathode and anode conditions, respectively. Obviously, this level is insufficient for an adequate operation of the corresponding electrodes, especially in reducing atmospheres which requires an improvement of current collection, for example, by fabrication of composites with metallic phases.

The electrode layers  $(\text{La}_{0.75}\text{Ca}_{0.25})_{0.95}\text{Cr}_{0.7}\text{Fe}_{0.3}\text{O}_{3-\delta}$  presented in Fig. 4 show a nonuniform porosity and particle size distribution, although one should not exclude a possibility of microstructural changes during the electrode testing. No cracks in the electrode layer or its delamination from the electrolyte was detected.

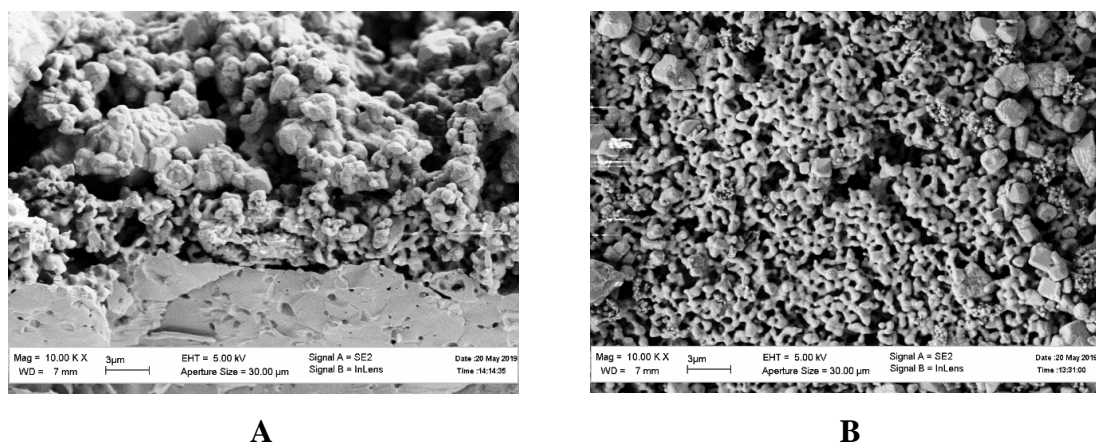


Fig. 4. Cross-section (A) and top view (B) of a cell with  $(\text{La}_{0.75}\text{Ca}_{0.25})_{0.95}\text{Cr}_{0.7}\text{Fe}_{0.3}\text{O}_{3-\delta}$  electrode layer after testing under anode conditions.

Fig. 5 demonstrates examples of the impedance spectra for  $(\text{La}_{0.75}\text{Ca}_{0.25})_{0.95}\text{Cr}_{0.7}\text{Fe}_{0.3}\text{O}_{3-\delta}$  and  $(\text{La}_{0.75}\text{Ca}_{0.25})_{0.95}\text{Cr}_{0.3}\text{Fe}_{0.7}\text{O}_{3-\delta}$  collected under cathodic and anodic conditions. For both electrodes, the Ohmic resistance decreases on increasing the oxygen partial pressure, in accordance with the electronic conductivity of the electrode materials. The polarization losses show a correlation with the content of the electrochemically-active component in the gas

mixture, i.e.  $O_2$  or  $H_2$  for cathode and anode conditions, respectively. While these effects are similar for both electrode compositions, the impact of Cr:Fe ratio differs for various testing conditions.  $(La_{0.75}Ca_{0.25})_{0.95}Cr_{0.3}Fe_{0.7}O_{3-\delta}$  cathode exhibits lower ohmic and polarization resistance compared to the material with higher Cr content; this trend is not surprising taking into account better conductivity of Fe-rich compositions (Fig. 3) and well-known improved catalytic activity of ferrite-based compositions towards redox processes [36-38]. The low-frequency arc for the Fe-enriched cathode is more suppressed (Fig. 5D) than that for  $(La_{0.75}Ca_{0.25})_{0.95}Cr_{0.7}Fe_{0.3}O_{3-\delta}$  which may be associated with microstructural factors or a mechanism of oxygen adsorption or surface diffusion promoted by the higher electronic and ionic conductivity. However, in reductive atmospheres introduction of iron into the electrode composition has a negative effect, in spite of higher conductivity compared to  $(La_{0.75}Ca_{0.25})_{0.95}Cr_{0.7}Fe_{0.3}O_{3-\delta}$  and negligible difference of the thermal and chemical expansion. One should note that the phase composition of  $(La_{0.75}Ca_{0.25})_{0.95}Cr_{0.3}Fe_{0.7}O_{3-\delta}$  annealed in similar  $H_2O$ - $H_2$ -Ar atmosphere exhibited no additional phases.

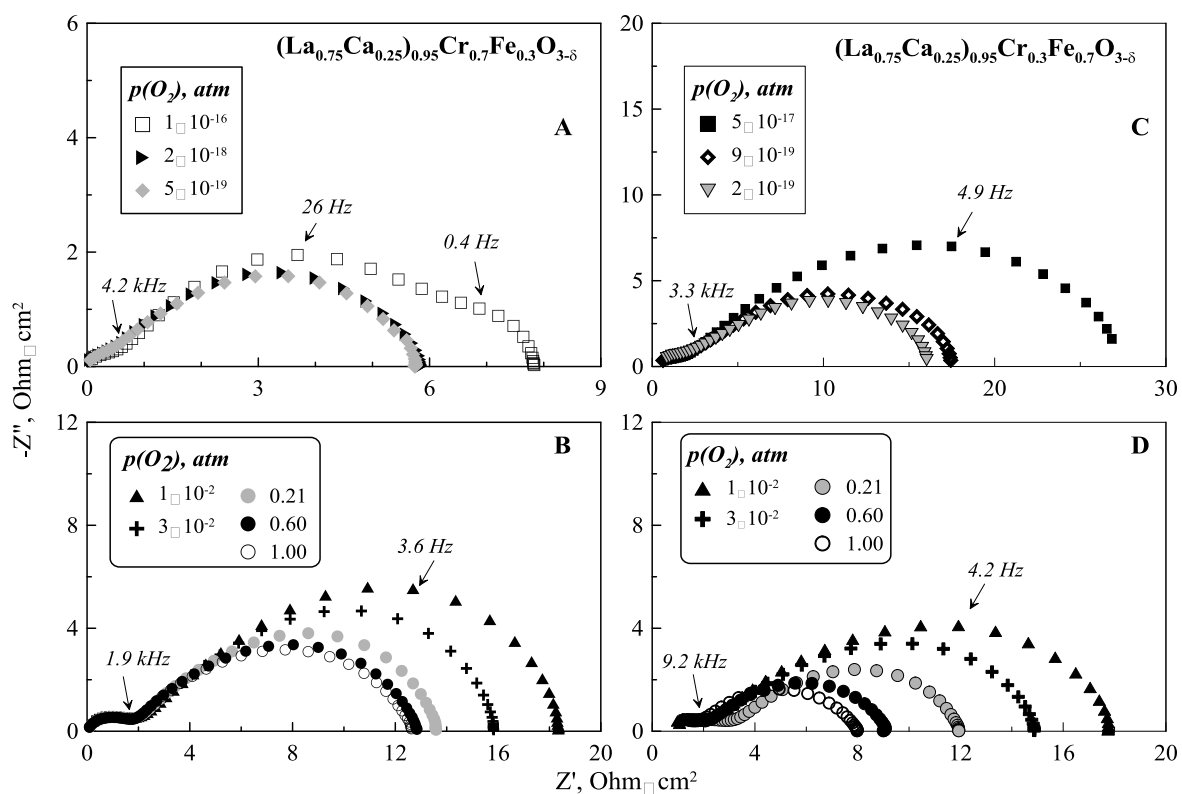


Fig. 5. Impedance spectra corrected for the electrode area and Ohmic resistance for  $(La_{0.75}Ca_{0.25})_{0.95}Cr_{0.7}Fe_{0.3}O_{3-\delta}$  (A, B) and  $(La_{0.75}Ca_{0.25})_{0.95}Cr_{0.3}Fe_{0.7}O_{3-\delta}$  (C, D) under reducing (A, C) and oxidizing (B, D) conditions.

As can be seen from Fig. 6, the activation energies of the electrode reactions both in reducing and oxidizing atmospheres are substantially higher for  $(\text{La}_{0.75}\text{Ca}_{0.25})_{0.95}\text{Cr}_{0.3}\text{Fe}_{0.7}\text{O}_{3-\delta}$  compared to the Cr-rich analogue, regardless of the opposite trends in the conductivity behavior. This fact suggests that at least for one electrode composition the electrochemical activity is governed by factors independent of the electronic supply/removal to/from the electrochemically-active sites. This suggestion is confirmed by substantially lower values of  $E_a$  for the total conductivity (Fig. 3) than those for the electrochemical activity. The observed trend is not typical for most perovskite-based electrode [2, 7, 8], where the electronic conductivity is considered to be the major performance-determined factor, and might be attributed to differences in the microstructure or excessive formation of oxygen vacancies on the surface of Fe-enriched perovskites leading to local ordering which influences the electrocatalytic properties. One should also take into account that the structural transition for  $(\text{La}_{0.75}\text{Ca}_{0.25})_{0.95}\text{Cr}_{0.7}\text{Fe}_{0.3}\text{O}_{3-\delta}$  occurs at  $\sim 815$  K, i.e. all the electrochemical tests were carried out on the material with rhombohedral or cubic structure. As for  $(\text{La}_{0.75}\text{Ca}_{0.25})_{0.95}\text{Cr}_{0.3}\text{Fe}_{0.7}\text{O}_{3-\delta}$ , the structural transformation occurred in the temperature range where the electrochemical studies were carried out which might substantially affect its electrochemical behavior.

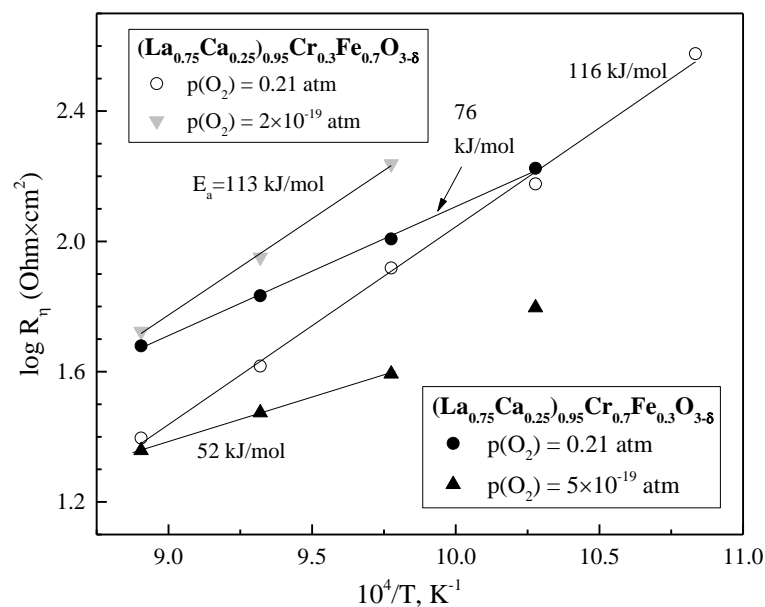


Fig. 6. Temperature dependencies of the polarization resistance of  $(\text{La}_{0.75}\text{Ca}_{0.25})_{0.95}\text{Cr}_{1-x}\text{Fe}_x\text{O}_{3-\delta}$  electrodes in  $\text{O}_2$  and wet 4%  $\text{H}_2$ -Ar atmospheres. The activation energies of the reciprocal total polarization resistance are marked near the corresponding data.

While decreasing hydrogen pressure over  $(\text{La}_{0.75}\text{Ca}_{0.25})_{0.95}\text{Cr}_{0.7}\text{Fe}_{0.3}\text{O}_{3-\delta}$  anode leads to an appearance of additional low-frequency semicircle (Fig. 5A) associated with retarded gas-phase diffusion, the  $(\text{La}_{0.75}\text{Ca}_{0.25})_{0.95}\text{Cr}_{0.3}\text{Fe}_{0.7}\text{O}_{3-\delta}$  anode demonstrates a substantial enlargement of the intermediate-frequency arc (Fig. 4C) suggesting a higher role of surface-associated processes. Obviously, this phenomenon deserves further studies. One should remind that increasing iron content in  $(\text{La}_{0.75}\text{Sr}_{0.25})_{0.95}\text{Cr}_{1-x}\text{Fe}_x\text{O}_{3-\delta}$  also resulted in worse electrochemical activity, presumably due to decreasing electronic conductivity [7]. Whatever the origins of such unexpected electrode behavior, the high level of the polarization resistance makes it necessary to modify the electrode composition, for instance, by fabrication of composite anodes, introduction of catalytically-active components or by a proper application of the current-collecting layer.

## Conclusions

Increasing iron content in  $(\text{La}_{0.75}\text{Sr}_{0.25})_{0.95}\text{Cr}_{1-x}\text{Fe}_x\text{O}_{3-\delta}$  perovskites leads to higher electronic conductivity, thermal expansion coefficient and electrochemical activity of the corresponding cathodes. Moreover, the temperature of the structural transition “orthorhombic” – “rhombohedral” shifts with Fe-doping towards higher temperatures. The influence of Cr:Fe ratio under anode conditions is, however, different to that for the conductivity at low  $p(\text{O}_2)$  indicating that other factors such as the structural transformation, anode microstructure or ordering of the surface oxygen vacancies are responsible for the anode behavior. The high values of the polarization resistance require optimization of the electrode layers.

## Acknowledgements

This work was supported by the Russian Science Foundation (grant 17-79-30071). The facilities and experimental technique for dilatometric tests in controlled atmospheres were developed with support by the State task of the Institute of Solid State Physics RAS.

## References

- [1] Jiang S.P., Chan S.H. A review of anode materials development in solid oxide fuel cells. *J. Mater. Sci.* 2004, vol. 39, iss. 14, pp. 4405-4439.
- [2] Tsipis E.V., Kharton V.V. Electrode materials and reaction mechanisms in solid oxide fuel cells: a brief review. III. Recent trends and selected methodological aspects. *J. Solid State Electrochem.* 2011, vol. 15, iss. 5, pp. 1007-1040.
- [3] McIntosh S., Gorte R.J. Recent developments on anodes for direct fuel utilization in SOFC. *Chem. Rev.* 2004, vol. 104, iss. 10, pp. 4845-4866.
- [4] Fergus J.W. Lanthanum chromite-based materials for solid oxide fuel cell interconnects. *Solid State Ionics.* 2004, vol. 171, iss. 1-2, pp. 1-15.
- [5] Tao S., Irvine J.T.S. Synthesis and Characterization of  $(\text{La}_{0.75}\text{Sr}_{0.25})\text{Cr}_{0.5}\text{Mn}_{0.5}\text{O}_{3-\delta}$ , a Redox-Stable, Efficient Perovskite Anode for SOFCs. *J. Electrochem. Soc.* 2004, vol. 151, iss. 2, pp. A252-A259.
- [6] Yasuda I., Hikita T. Electrical Conductivity and Defect Structure of Calcium- Doped Lanthanum Chromites. *J. Electrochem. Soc.* 1993, vol. 140, iss. 6, pp. 1699-1704.
- [7] Lü M.F., Tsipis E.V., Waerenborgh J.C., Yaremchenko A.A., Kolotygin V.A., Bredikhin S., Kharton V.V. Thermomechanical, transport and anodic properties of perovskite-type  $(\text{La}_{0.75}\text{Sr}_{0.25})_{0.95}\text{Cr}_{1-x}\text{Fe}_x\text{O}_{3-\delta}$ . *J. Power Sources.* 2012, vol. 206, pp. 59-69.
- [8] Kolotygin V.A., Tsipis E.V., Lü M.F., Pivak Y.V., Yarmolenko S.N., Bredikhin S.I., Kharton V.V. Functional properties of SOFC anode materials based on  $\text{LaCrO}_3$ ,  $\text{La}(\text{Ti},\text{Mn})\text{O}_3$  and  $\text{Sr}(\text{Nb},\text{Mn})\text{O}_3$  perovskites: A comparative analysis. *Solid State Ionics.* 2013, vol. 251, pp. 28-33.
- [9] Kobsiriphat W., Madsen B.D., Wang Y., Marks L.D., Barnett S.A.  $\text{La}_{0.8}\text{Sr}_{0.2}\text{Cr}_{1-x}\text{Ru}_x\text{O}_{3-\delta}-\text{Gd}_{0.1}\text{Ce}_{0.9}\text{O}_{1.95}$  solid oxide fuel cell anodes: Ru precipitation and electrochemical performance. *Solid State Ionics.* 2009, vol. 180, iss. 2-3, pp. 257-264.
- [10] Danilovic N., Vincent A., Luo J.L., Chuang K.T., Hui R., Sanger A.R. Correlation of Fuel Cell Anode Electrocatalytic and ex situ Catalytic Activity of Perovskites  $\text{La}_{0.75}\text{Sr}_{0.25}\text{Cr}_{0.5}\text{X}_{0.5}\text{O}_{3-\delta}$  ( $\text{X} = \text{Ti}, \text{Mn}, \text{Fe}, \text{Co}$ ). *Chem. Mater.* 2009, vol. 22, iss. 3, pp. 957-965.
- [11] Peña-Martínez J., Marrero-López D., Pérez-Coll D., Ruiz-Morales J.C., Núñez P. Performance of  $\text{XSCoF}$  ( $\text{X} = \text{Ba}, \text{La}$  and  $\text{Sm}$ ) and  $\text{LSCrX'}$  ( $\text{X'} = \text{Mn}, \text{Fe}$  and  $\text{Al}$ ) perovskite-structure materials on LSGM electrolyte for IT-SOFC. *Electrochim. Acta.* 2007, vol. 178, iss. 9, pp. 101-113.

- [12] Kharton V.V., Tsipis E.V., Marozau I.P., Viskup A.P., Frade J.R., Irvine J.T.S. Mixed conductivity and electrochemical behavior of  $(\text{La}_{0.75}\text{Sr}_{0.25})_{0.95}\text{Cr}_{0.5}\text{Mn}_{0.5}\text{O}_{3-\delta}$ . *Solid State Ionics*. 2007, vol. 178, iss. 1-2, pp. 101-113.
- [13] Jiang S.P., Ye Y., He T., Ho S.B. Nanostructured palladium- $\text{La}_{0.75}\text{Sr}_{0.25}\text{Cr}_{0.5}\text{Mn}_{0.5}\text{O}_3/\text{Y}_2\text{O}_3\text{-ZrO}_2$  composite anodes for direct methane and ethanol solid oxide fuel cells. *J. Power Sources*. 2008, vol. 185, iss. 1, pp. 179-182.
- [14] Tan W., Zhong Q., Xu D., Yan H., Zhu X. Catalytic activity and sulfur tolerance for Mn-substituted  $\text{La}_{0.75}\text{Sr}_{0.25}\text{CrO}_{3\pm\delta}$  in gas containing  $\text{H}_2\text{S}$ . *Int. J. Hydr. Energy*. 2013, vol. 38, iss. 36, pp. 16656-16664.
- [15] Ruiz-Morales J.C., Canales-Vázquez, J.Ballesteros-Pérez B., Peña-Martínez J., Marrero-López D., Irvine J.T.S., Núñez P. LSCM-(YSZ-CGO) composites as improved symmetrical electrodes for solid oxide fuel cells. *J. Eur. Ceram. Soc.* 2007, vol. 27, iss. 13-15, pp. 4223-4227.
- [16] Yuan C., Zhou Y., Qian J., Ye. X., Zhan Z., Wang S.,  $\text{La}_{0.8}\text{Sr}_{0.2}\text{Cr}_{0.5}\text{Fe}_{0.5}\text{O}_{3-\delta}$  as anode material on cathode-support SOFCs for direct hydrocarbon utilization. *Mater. Res. Innovations*. 2014, vol. 18, suppl. 4, pp. 132-136.
- [17] Lai K.Y., Manthiram A., Self-Regenerating Co-Fe Nanoparticles on Perovskite Oxides as a Hydrocarbon Fuel Oxidation Catalyst in Solid Oxide Fuel Cells. *Chem. Mater.* 2018, vol. 30, iss. 8, pp. 2515-2525.
- [18] Wei T., Zhou X., Hu Q., Gao Q., Han D., Lv X., Wang S. A high power density solid oxide fuel cell based on nano-structured  $\text{La}_{0.8}\text{Sr}_{0.2}\text{Cr}_{0.5}\text{Fe}_{0.5}\text{O}_{3-\delta}$  anode. *Electrochim. Acta*. 2014, vol. 148, pp. 33-38.
- [19] Gong M., Bierschenk D., Haag J., Poeppelmeier K.R., Barnett S.A., Xu C., Zondlo J.W., Liu X. Degradation of  $\text{LaSr}_2\text{Fe}_2\text{CrO}_{9-\delta}$  solid oxide fuel cell anodes in phosphine-containing fuels. *J. Power Sources*. 2010, vol. 195, iss. 13, pp. 4013-4021.
- [20] Chesnokov K.Yu., Markov A.A., Patrakeeve M.V., Leonidov I.A., Murzakaev A.M., Leonidova O.N., Shalaeva E.V., Kharton V.V., Kozhevnikov V.L. Structure and transport properties of  $\text{La}_{0.5}\text{Sr}_{0.5-x}\text{Ca}_x\text{FeO}_{3-\delta}$ . *Solid State Ionics*. 2014, vol. 262, pp. 672-677.
- [21] Kolotygin V.A., Tsipis E.V., Patrakeeve M.V., Waerenborgh J.C., Kharton V.V. Time degradation of electronic and ionic transport in perovskite-like  $\text{La}_{0.5}\text{Ca}_{0.5}\text{FeO}_{3-\delta}$ . *Mater. Lett.* 2019, vol. 239, pp. 167-171.
- [22] Kolotygin V.A., Tsipis E.V. Patrakeeve M.V., Ivanov A.I., Kharton V.V. Stability, mixed conductivity, and thermomechanical properties of perovskite materials for fuel cell electrodes

based on  $\text{La}_{0.5}\text{A}_{0.5}\text{Mn}_{0.5}\text{Ti}_{0.5}\text{O}_{3-\delta}$ ,  $\text{La}_{0.5}\text{Ba}_{0.5}\text{Ti}_{0.5}\text{Fe}_{0.5}\text{O}_{3-\delta}$ , and  $(\text{La}_{0.5}\text{A}_{0.5})_{0.95}\text{Cr}_{0.5}\text{Fe}_{0.5}\text{O}_{3-\delta}$  ( $\text{A} = \text{Ca}, \text{Ba}$ ). *Russ. J. Electrochem.* 2016, vol. 52, iss. 7, pp. 628-641.

[23] Shannon R.D. Revised Effective Ionic Radii and Systematic Studies of Interatomic Distances in Halides and Chalcogenides. *Acta Cryst.* 1976, vol. A32, pp. 751-767.

[24] Kolotygin V.A., Tsipis E.V., Markov A.A., Patrakeev M.V., Waerenborgh J.C., Shaula A.L., Kharton V.V. Transport and Electrochemical Properties of  $\text{SrFe}(\text{Al}, \text{Mo})\text{O}_{3-\delta}$ . *Russ. J. Electrochem.* 2018, vol. 54, iss. 6, pp. 514-526.

[25] Kharton V.V., Yaremchenko A.A., Patrakeev M.V., Naumovich E.N., Marques F.M.B. Thermal and chemical induced expansion of  $\text{La}_{0.3}\text{Sr}_{0.7}(\text{Fe}, \text{Ga})\text{O}_{3-\delta}$  ceramics. *J. Eur. Ceram. Soc.* 2003, vol. 23, iss. 9, pp. 1417-1426.

[26] Yaremchenko A.A., Kharton V.V., Kolotygin V.A., Patrakeev M.V., Tsipis E.V., Waerenborgh J.C. Mixed conductivity, thermochemical expansion and electrochemical activity of Fe-substituted  $(\text{La}, \text{Sr})(\text{Cr}, \text{Mg})\text{O}_{3-\delta}$  for solid oxide fuel cell anodes. *J. Power Sources.* 2014, vol. 249, pp. 483-496.

[27] Mori M., Yamamoto T., Itoh H., Watanabe T. Compatibility of alkaline earth metal (Mg, Ca, Sr)-doped lanthanum chromites as separators in planar-type high-temperature solid oxide fuel cells. *J. Mater. Sci.* 1997, vol. 32, iss. 9, pp. 2423-2431.

[28] Höfer H.E., Schmidberger R. Electronic Conductivity in the  $\text{La}(\text{Cr}, \text{Ni})\text{O}_3$  Perovskite System. *J. Electrochem. Soc.* 1994, vol. 141, iss. 3, pp. 782-786.

[29] Kharton V.V., Yaremchenko A.A., Naumovich E.N. Research on the electrochemistry of oxygen ion conductors in the former Soviet Union. II. Perovskite-related oxides. *J. Solid State Electrochem.* 1999, vol. 3, iss. 6, pp. 303-326.

[30] Yarmolenko S., Gordon K., Hancock B., Kharton V., Sankar J. Characterization of  $(\text{La}_{0.9}\text{Sr}_{0.1})_{0.95}\text{Cr}_{0.85}\text{Mg}_{0.10}\text{Ni}_{0.05}\text{O}_{3-\delta}$  Ceramics for Perovskite Related Membrane Reactor. *ASME 2007 International Mechanical Engineering Congress and Exposition.* 2007, vol. 13, pp. 215-223.

[31] Kharton V.V., Marques F.M.B., Atkinson A. Transport properties of solid oxide electrolyte ceramics: a brief review. *Solid State Ionics.* 2004, vol. 174, iss. 1-4, pp. 135-149.

[32] Raffaele B., Anderson H.U., Sparlin D.M., Parris P.E. Transport anomalies in the high-temperature hopping conductivity and thermopower of Sr-doped  $\text{La}(\text{Cr}, \text{Mn})\text{O}_3$ . *Phys. Rev. B.* 1991, vol. 43, pp. 7991-7999.

[33] Koc R., Anderson H.U. Electrical and thermal transport properties of  $(\text{La}, \text{Ca})(\text{Cr}, \text{Co})\text{O}_3$ . *J. Eur. Ceram. Soc.* 1995, vol. 15, iss. 9, pp. 867-874.

- [34] Vashook V., Vasylechko L., Zosel J., Gruner W., Ullmann H., Guth U. Crystal structure and electrical conductivity of lanthanum–calcium chromites–titanates  $\text{La}_{1-x}\text{Ca}_x\text{Cr}_{1-y}\text{Ti}_y\text{O}_{3-\delta}$  ( $x=0-1$ ,  $y=0-1$ ). *J. Solid State Chem.* 2004, vol. 177, iss. 10, pp. 3784-3794.
- [35] Koc R., Anderson H.U. Investigation of strontium-doped  $\text{La}(\text{Cr},\text{Mn})\text{O}_3$  for solid oxide fuel cells. *J. Mater. Sci.* 1992, vol. 27, iss. 21, pp. 5837-5843.
- [36] Markov A.A., Patrakeeve M.V., Leonidov I.A., Kozhevnikov V.L. Reaction control and long-term stability of partial methane oxidation over an oxygen membrane. *J. Solid State Electrochem.* 2011, vol. 15, iss. 2, pp. 253-257.
- [37] Yaremchenko A.A., Kharton V.V., Valente A.A., Snijkers F.M.M., Coymans J.F.C., Luyten J.J., Marques F.M.B. Performance of tubular  $\text{SrFe}(\text{Al})\text{O}_{3-\delta}$ - $\text{SrAl}_2\text{O}_4$  composite membranes in  $\text{CO}_2$ - and  $\text{CH}_4$ -containing atmospheres. *J. Membr. Sci.* 2008, vol. 319, iss. 1-2, pp. 141-148.
- [38] Fischer II J.C., Chuang S.S.C. Investigating the  $\text{CH}_4$  reaction pathway on a novel LSCF anode catalyst in the SOFC. *Catal. Commun.* 2009, vol. 10, iss. 6, pp. 772-776.



# Перовскитоподобные $(\text{La}_{0.75}\text{Ca}_{0.25})_{0.95}\text{Cr}_{1-x}\text{Fe}_x\text{O}_{3-\delta}$ для потенциального использования в качестве электродных материалов симметричных Твердооксидных Топливных Элементов

В.А. Колотыгин, А.И. Иванов, Н.Б. Кострцова, В.В. Хартон

## Аннотация

Работа посвящена синтезу и аттестации перовскитов  $(\text{La}_{0.75}\text{Ca}_{0.25})_{0.95}\text{Cr}_{1-x}\text{Fe}_x\text{O}_{3-\delta}$  в качестве потенциальных катодов и анодов ТОТЭ. Для материалов характерна орторомбическая структура на воздухе, в то время как при нагреве выше 800-1100 К происходит обратимый переход структуры в ромбоэдрическую симметрию. Температура перехода растет с содержанием железа. Значения линейного коэффициента термического расширения изменяются в интервале  $(10.5-11.1) \times 10^{-6} \text{ K}^{-1}$ , слегка увеличиваясь при легировании материалов железом, в то время как объемные изменения при восстановлении не превышают 0.16%. Электронная проводимость проявляет термически-активированный характер и увеличивается при введении железа, предположительно благодаря росту числа узлов доступных для электронного переноса. Данное поведение наблюдается в окислительных и восстановительных условиях. Низкий уровень электронной проводимости предположительно обуславливает недостаточно высокую каталитическую активность катодов на основе  $(\text{La}_{0.75}\text{Ca}_{0.25})_{0.95}\text{Cr}_{1-x}\text{Fe}_x\text{O}_{3-\delta}$ , в то время как в анодных условиях электрохимическое поведение связано с рядом других факторов, таких как электродная микроструктура или поверхностные явления.

**Ключевые слова:** перовскит, фазовый переход, термическое расширение, химическое расширение, полная электропроводность, поляризационное сопротивление.